

Spectrally resolved white-light phase-shifting interference microscopy for thickness-profile measurements of transparent thin film layers on patterned substrates

Sanjit K. Debnath and Mahendra P. Kothiyal

Department of Physics, Indian Institute of Technology Madras, Chennai – 600 036, India
sanjit@physics.iitm.ac.in kothiyal@iitm.ac.in

Joanna Schmit

Veeco Instruments Inc., 2650 East Elvira Road, Tucson, AZ 85711, USA
jschmit@veeco.com

Parameswaran Hariharan

School of Physics, University of Sydney, NSW 2006, Australia
hariharan_optics@hotmail.com

Abstract: We describe how spectrally-resolved white-light phase-shifting interference microscopy with a windowed 8-step algorithm can be used for rapid and accurate measurements of the thickness profile of transparent thin film layers with a wide range of thicknesses deposited upon patterned structures exhibiting steps and discontinuities. An advantage of this technique is that it can be implemented with readily available hardware.

©2006 Optical Society of America

OCIS codes: (120.3180) Interferometry; (120.5050) Phase measurement; (120.6200) Spectrometers and spectroscopic instrumentation; (240.0310) Thin films

Reference and links

1. S. S. C. Chim and G. S. Kino, "Correlation microscope," *Opt. Lett.* **15**, 579-581 (1990).
2. B. S. Lee and T. C. Strand, "Profilometry with a coherence scanning microscope," *Appl. Opt.* **29**, 3784-3788 (1990).
3. P. Hariharan and M. Roy, "White-light phase-stepping interferometry for surface profiling," *J. Mod. Opt.* **41**, 2197-2201 (1994).
4. P. Hariharan and M. Roy, "Interferometric surface profiling with white light: effect of surface films," *J. Mod. Opt.* **43**, 1797-1800 (1996).
5. S. W. Kim and G. H. Kim, "Thickness profile measurement of transparent thin-film layers by white-light scanning interferometry," *Appl. Opt.* **38**, 5968-5973 (1999).
6. D. Kim and S. Kim, "Direct spectral phase function calculation for dispersive interferometric thickness profilometry," *Opt. Express*, **12**, 5117-5124 (2004).
7. D. Kim, S. Kim, H. Kong and Y. Lee, "Measurement of the thickness profile of a transparent thin film deposited upon a pattern structure with an acousto-optic tunable filter," *Opt. Lett.* **27**, 1893-1895 (2002).
8. J. Calatroni, A. L. Guerrero, C. Sainz and R. Escalona, "Spectrally resolved white-light interferometry as a profilometry tool," *Opt. Laser Technol.* **28**, 485-489 (1996).
9. P. Sandoz, G. Tribillon and H. Perrin, "High resolution profilometry by using phase calculation algorithms for spectroscopic analysis of white light interferograms," *J. Mod. Opt.* **43**, 701-708 (1996).
10. S. S. Helen, M. P. Kothiyal and R. S. Sirohi, "Analysis of spectrally resolved white light interferograms: use of a phase shifting technique," *Opt. Eng.* **40**, 1329-1336 (2001).
11. S. K. Debnath and M. P. Kothiyal, "Optical profiler based on spectrally resolved white light interferometry," *Opt. Eng.* **44**, 013606 (2005).
12. P. Hariharan, B. F. Oreb and T. Eiju, "Digital phase-shifting interferometry: a simple error-compensating phase calculation algorithm," *Appl. Opt.* **26**, 2504-2506 (1987).
13. J. Schmit and K. Creath, "Extended averaging technique for derivation of error-compensating algorithms in phase-shifting interferometry," *Appl. Opt.* **34**, 3610-3619 (1995).

14. J. Schmit and K. Creath, "Window function influence on phase error in phase-shifting algorithms," *Appl. Opt.* **35**, 5642-5649 (1996).
15. M. Born and E. Wolf, *Principles of Optics*, 7th Ed. (Cambridge University Press, 1999), pp. 752-758.
16. A. Harasaki and J. C. Wyant, "Fringe modulation skewing effect in white light vertical scanning interferometry," *Appl. Opt.* **39**, 2101-2106 (2000).

1. Introduction

An area of increasing importance in the optoelectronics industry is the development of non-contact techniques for rapidly and accurately mapping micromachined surfaces. Laser interferometry permits very precise measurements but has the disadvantage that it only yields the fractional interference order at each point. As a result, ambiguities may arise at discontinuities or steps involving a change in height greater than half the laser wavelength.

One way to overcome the problem of ambiguities is by using white light and scanning the object in depth. The position along the depth axis corresponding to maximum fringe visibility (the coherence peak) for each pixel in the image can be located by using Fourier transforms [1, 2] or by other techniques such as achromatic phase-shifting. [3]

A problem is that, in many cases, transparent film layers are deposited on these patterned structures, making it difficult to obtain accurate 3-D surface profiles. [4] This problem can be solved and the 3-D volumetric thickness profiles of such structures obtained by measurements of the spectral phase function at an array of points using Fourier transforms. [5, 6] However, the Fourier transform method has the disadvantages of complexity and long computation time. A faster and more direct way to obtain the spectral phase function is by using spectral scanning and phase shifting. The major drawback of this technique is that it involves using a spectral scanning device, such as an acousto-optic tunable filter, to make a series of measurements of the phase difference between the beams, at an array of points, at a number of wavelengths. [7]

2. Spectrally-resolved phase-shifting interference microscopy

An alternative technique that has been used with a white-light source to obtain unambiguous values of the phase difference along a line is spectrally-resolved white-light interferometry (SRWLI). [8, 9] In this technique, the interferogram is imaged on the slit of a spectroscopy which is used to analyze the light from each point on the slit. The phase difference between the beams, at each point on the object along the line defined by the slit can then be obtained from the intensity distribution in the resulting channeled spectrum. Much higher accuracy can be obtained by phase shifting, using an achromatic phase-shifter operating on the Pancharatnam phase, [10] however, this technique requires specialized hardware.

In this paper we have discussed the use of the conventional piezoelectric translator (PZT) phase shifting for this application. With a conventional PZT, the phase shift is wavelength dependent. As a result only the pixel receiving the design wavelength will experience the design phase shift. However, it has been shown that good results can be obtained with a PZT phase shifter by using a five-step algorithm that is comparatively insensitive to phase-step errors. [11,12] Since we need accurate measurements of small deviations from linearity of the spectral phase function, a high degree of insensitivity to phase-step miscalibration is desirable. We have, therefore, employed an algorithm using eight phase steps with a nominal value of 90° and a bell-shaped window function, [13, 14] which can be written in the form

$$\tan \phi = \frac{-I_1 - 5I_2 + 11I_3 + 15I_4 - 15I_5 - 11I_6 + 5I_7 + I_8}{I_1 - 5I_2 - 11I_3 + 15I_4 + 15I_5 - 11I_6 - 5I_7 + I_8} \quad (1)$$

With this algorithm, the errors in the measured phase are less than 0.01° for a phase-step error of 20° . In addition, this algorithm exhibits a high degree of insensitivity to detector nonlinearities and other sources of error.

The values of the phase ϕ (modulo 2π), obtained as a function of the wave number σ , are easily unwrapped, because we know that ϕ is a continuous function of σ . Errors due to

variations in the sensitivity of different pixels are avoided, since the intensity values used for calculating the phase at each wavelength are obtained from the same pixel. A resolution of 1 nm in height is possible.

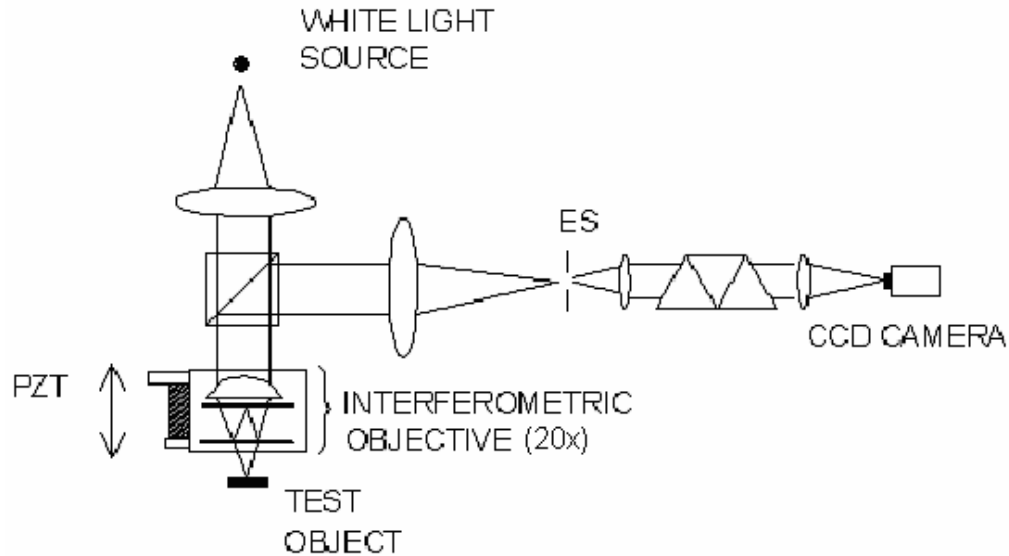


Fig. 1. Schematic of the spectrally-resolved phase-shifting interference profilometer.

With this technique, the values of the phase difference obtained at a series of pixels along the direction of dispersion (corresponding to a number of different wavelengths) yield a direct measurement of the spectral phase function at the sampled point. A single set of measurements can, therefore, be used to generate a thickness profile along the line defined by the slit. Such a profile along a line is adequate for many applications.

3. Experimental arrangement

The experimental setup used for spectrally resolved white light phase shifting interferometry is shown in Fig. 1. The test surface is observed through a Mirau-type interferometric microscope objective (20x). The light source is a tungsten-halogen lamp with a broad continuous spectrum. The white-light interferogram of the surface, formed at the exit plane of the microscope, is imaged on the entrance slit (ES) of a direct vision spectroscope. The entrance slit selects a line on the test surface for profiling. The output of the spectroscope (wavelength range 458 nm to 783 nm) is received on a CCD camera, which is aligned with the columns of pixels parallel to the entrance slit (ES). Because the dispersion of the spectroscope is perpendicular to the slit, the rows correspond to the wave-number axis. The camera (Pulnix 1010) gives a 10-bit digital output. The interferograms are transferred to a PC through an image acquisition board (NI PCI 1422). Phase shifting is accomplished by fitting the objective mount with a PZT. The control voltage applied to the PZT for phase shifting is produced by a digital-to-analog card (NI DAQ). A cadmium spectral lamp is used for wavelength calibration of the CCD camera pixels. [11]

The intensity at a point (x, σ) in the dispersed fringe pattern captured by the CCD array detector can be written as [6]

$$I(x, \sigma) = I_0(x, \sigma) [1 + V(x, \sigma) \cos\phi(x, \sigma)] \quad (2)$$

where I_0 is the average intensity in the interference pattern, V is the visibility function, x is the distance from one end of the slit and $\sigma = 1/\lambda$ is the wave number. The phase function $\phi(x, \sigma)$, which can be evaluated directly for all values of x and σ by phase-shifting, as described

earlier, then contains, for each value of x , the corresponding value of the spectral phase function $\phi(\sigma)$.

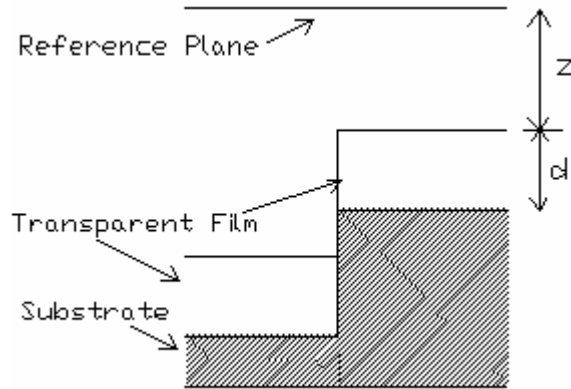


Fig. 2. Cross section of a patterned surface with a transparent film deposited on it.

If, as shown in Fig. 2, we have a transparent thin film deposited on a patterned structure, the phase function $\phi(x, \sigma)$ can be written in the form

$$\phi(x, \sigma) = 4\pi\sigma z(x) + \psi(\sigma, x, d, n_2), \quad (3)$$

where z represents the distance from the reference plane to the top surface of the transparent film, d and n_2 represent, respectively, the thickness and refractive index of the transparent film, and $\psi(\sigma, x, d, n_2)$ represents a phase term due to the film that can be modeled using the theory of thin films. [15] The first term on the right-hand side of Eq. (3), which is the phase term due to the air gap, is a linear function of σ . A simulation of the phase $\psi(\sigma)$ of a typical SiO_2 film ($1.5 \mu\text{m}$ thick) on a silicon substrate is shown in Fig. 3. It is apparent that there is a significant linear part (ϕ_l) of the phase, which is proportional to the film thickness ($\phi_l \approx 4\pi n_2 \sigma d$). The nonlinear part (ϕ_{nl}) is the contribution of multiple reflections. Hence, Eq. (3) may be written as

$$\phi(x, \sigma) = 4\pi\sigma z + 4\pi n_2 \sigma d + \phi_{nl} \quad (4)$$

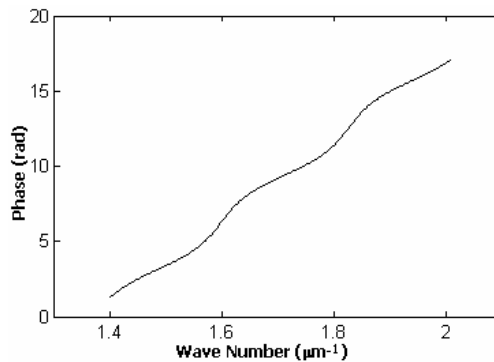


Fig. 3. Simulated phase ψ for a $1.5 \mu\text{m}$ SiO_2 film on Si.

Equation (4) suggests that the slope of a linear fit to the $\phi(x, \sigma)$ vs. σ data will give a good estimate of the quantity $4\pi(z + n_2 d)$. The thickness profile can then be obtained by a least-squares fit to the actual phase data. This is done by finding, for each value of x , the values of z and d which minimize the error function

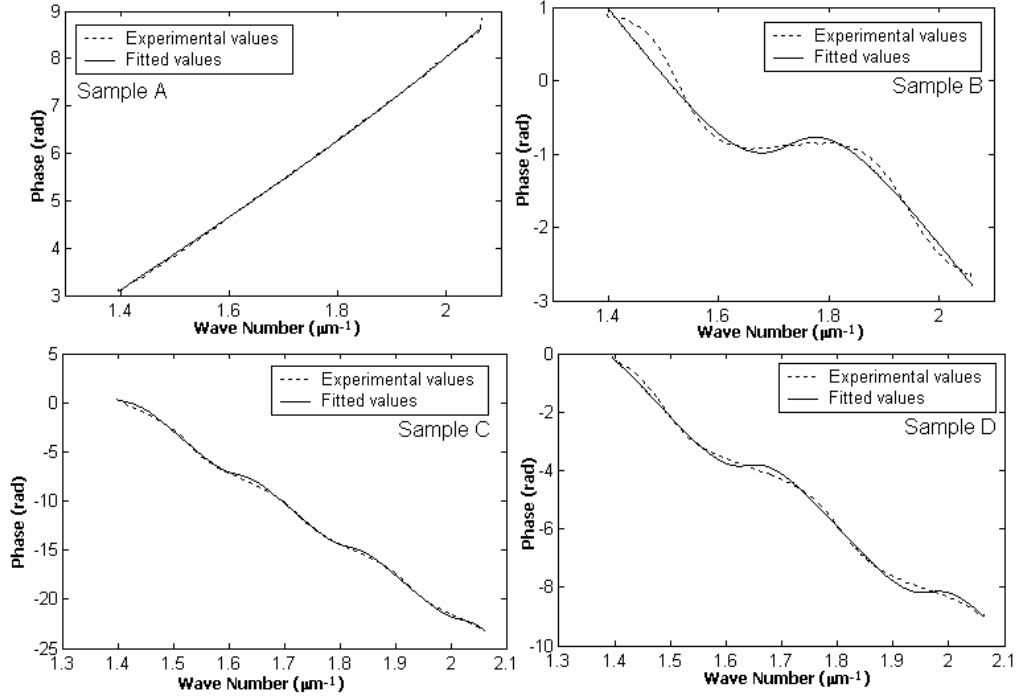


Fig. 4. Phase $\phi(x, \sigma)$ vs. wave number σ at a point on the surface for four Si samples with SiO_2 films of different thicknesses.

$$\eta(z, d) = \sum [\phi_{\text{model}}(\sigma, z, d) - \phi_{\text{measured}}(\sigma)]^2 \quad (5)$$

4. Measurements and results

Experiments were carried out with three plane silicon wafer samples with SiO_2 films of different thicknesses (samples A, B, C), as well as with a patterned silicon wafer with a SiO_2 film (sample D). Eight phase shifted interferograms were recorded of the dispersed fringe pattern, corresponding to phase steps of 90° produced by the PZT phase shifter at a wavelength of 610 nm. The phase at a series of points along the wave-number axis was calculated using Eq. (1). These values of the phase were unwrapped and the surface height and the thickness of the layer at each point, as given by Eq. (3), were then modeled so as to minimize the error function η given by Eq. (5). For simplicity, we assumed the values of the refractive index of SiO_2 ($n_2=1.46$) and the refractive index of Si ($n_1=3.85 - 0.02i$) to be independent of the wavelength. Where necessary, a better fit and higher accuracy can be obtained if the spectral variation of the refractive indexes is taken into account.

Initially we used a linear fit to the experimental data; the slope of this phase $\phi(x, \sigma)$ vs wave number line gives us an approximate value of $(z + n_2d)$ since, as mentioned above,

$$(z + n_2d) = \text{slope} / (4\pi) \quad (6)$$

We then used the Levenberg–Marquardt nonlinear least-squares fitting algorithm (Matlab) for thickness modeling. This algorithm requires an initial guess for d , which also gives us, from Eq. (6), an initial guess for z . With these values of d , z and the refractive index as inputs, we obtain, as the output, independently adjusted values of d and z which yield the best fit to the experimental values of the phase. Figure 4 shows the experimentally determined, and the best fitted, phase $\phi(x, \sigma)$ vs. wave number σ curves for four samples with films of different thicknesses.

For the four samples A, B, C and D the values of d and z , at the object point used for Fig. 4, are (151, 457), (595, -1266), (1697, -5383) and (1044, -2575) nm, respectively, with an estimated uncertainty of ± 5 nm. However, the results for the thickness vary over the scan length in the ranges (143 to 153), (594 to 596), (1694 to 1697) and (1043, 1053) nm, respectively. The corresponding average values of the thickness are 152 nm, 595 nm, 1696 nm and 1048 nm. The values of d and z are available at all the pixels along the scan line, which, with a 20x objective, is about $400 \mu\text{m}$ long. With these values of z and d , we can plot the profile of the top surface of the film, as well as the profile of the substrate, along the scan line. Figure 5 shows profiles obtained for the top surface of the film and the substrate for the four samples for which the phase is shown in Fig. 4. Samples 5A, 5B, 5C are plane Si wafers coated with SiO_2 films, while sample D is a patterned Si wafer coated with a SiO_2 film. The height of the step on sample D was found to be 479 nm. The distortion of the profile at the edges of the step seen with sample D is due to diffraction effects, which are a common problem in interference profilometry. [16]

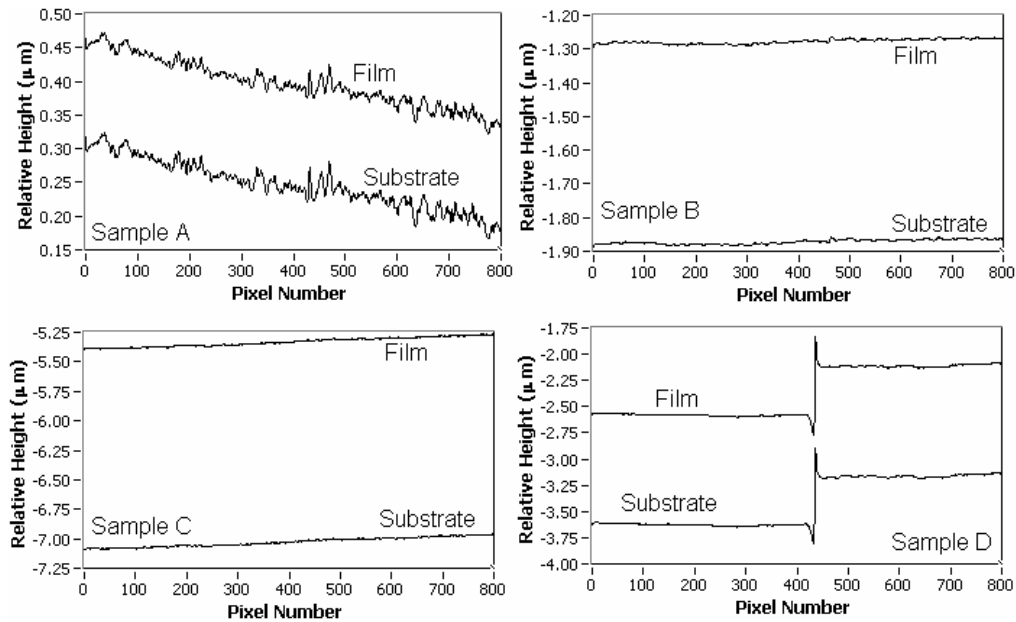


Fig. 5. Line profiles of the top surface of the film and substrate.

5. Conclusion

Spectrally-resolved white-light phase-shifting interference microscopy with a windowed 8-step algorithm can be used for rapid and accurate measurements of the thickness profile of transparent thin film layers, with thicknesses ranging from a few micrometers down to as low as 150 nm, deposited upon patterned structures exhibiting steps and discontinuities. A thickness profile along a line can be generated from a single set of measurements. Such a profile is adequate for many applications. Since data on the spectral phase function, at each point on the object, are obtained for a very large number of wavelengths, thickness profiles can be evaluated from a polynomial fit with high accuracy. This technique also has the advantage that it can be implemented with readily available hardware.